This manuscript was accepted by Rev. Sci.Instrum. Click here to see the version of record.

MIRRORS: a MATLAB® GUI for temperature measurement by multispectral imaging radiometry

O. T. Lord[1] and W. Wang[2]

[1]*School of Earth Sciences, University of Bristol, Wills Memorial Building, Queen's Road, Bristol, BS8 1RJ, UK*

[2]*Innovative Technology and Science Ltd, North Wing, Old Livery, Hildersham Road, Cambridge, CB21 6DR, UK*

Abstract. MIRRORS is an open source MATLAB based Graphical User Interface designed to automatically process images generated from a four colour multispectral imaging radiometry system for the temperature measurement of samples heated in a diamond anvil cell. The GUI can work in either a live mode (during an experiment) or in a post-processing mode, and performs background subtraction, spatial correlation and thermal calibration of the data before producing maps of temperature, emissivity, their associated uncertainties, an image difference map (i.e. the change in the shape of the temperature field) and a variety of other visualisations derived from them. We describe the distribution, system requirements and required hardware specific code modifications necessary to setup MIRRORS. We also describe the workflow of the software, its underlying methodologies and provide example output as well as the results of benchmarking against a traditional spectroradiometric system of known accuracy.

I. INTRODUCTION

The diamond anvil cell (DAC), combined with laser heating (LH) or resistive heating (RH) is the only device capable of accessing all pressure-temperature loci along the Earth's geotherm while maintaining a static sample environment[1]. This technology has been implemented by experimental petrologists, materials scientists and physicists at numerous laboratories and synchrotron beamlines concerned with the study of materials at extreme conditions. Precise and accurate determination of pressure and temperature are vital if the measurements of thermoelastic parameters, transport properties and phase equilibria in DAC experiments are to be useful. Temperature measurement is doubly important because uncertainties in pressure are correlated with uncertainties in temperature via thermal pressure caused by thermal expansion within the nearly isochoric sample chamber of the DAC.

Traditionally, temperature measurement in the DAC has been performed using spectroradiometry, where the light from the region of interest (ROI) is selected using a pinhole and dispersed onto a CCD by means of a spectrometer[2,3]. The resulting spectrum, calibrated against a source of known spectral intensity, is fitted using the Planck function or its Wien approximation, with the assumption that the emissivity of the sample is independent of wavelength, yielding the temperature of the ROI. Employing a slit instead of an aperture and a 2D CCD chip allows a 1D temperature profile to

be determined[2]. These methods can be extremely precise if implemented properly, with analytical uncertainties on the fitted spectra of a few K at sample temperatures of >2000 K[3]. In the ideal case of a radially symmetric hotspot and perfect alignment between its peak and the aperture, such a system will faithfully record both the peak temperature and the gradient, allowing the full 2D temperature field to be reconstructed. However, in most real experiments the heterogenous absorption characteristics of the sample can drive the temperature field far from this ideal case, and the aperture and the hotspot can easily become misaligned. In this situation, the peak temperature can be underestimated and the true temperature field cannot be reconstructed, leading to significant uncertainty in both the peak and average sample temperatures[4]. This is particularly problematic when trying to interpret the results of *in situ* analyses using X-ray diffraction or spectroscopy, where precise knowledge of the average temperature of the interaction volume of the X-ray probe can only be known if the spectroradiometric aperture and X-ray beam are perfectly co-aligned[5]. It also makes the interpretation of two-dimensional *ex situ* chemical maps difficult, given that we have no knowledge of the sample temperature beyond the limits of the aperture.

Recently, new methods have been employed that provide 2D temperature maps of hot DAC samples, circumventing these limitations and providing richer information about the dynamic changes occurring at high temperature[6]. In the peak-scaling method[5,7,8] a pseudo-Planck curve is measured using a spectrometer with a wide entrance slit that averages the light from the entire ROI. This pseudo-Planck curve is then corrected to determine a peak temperature which is used to scale a monochromatic image of the sample collected simultaneously on a CCD, resulting in a temperature map. This method is relatively simple to implement and is insensitive to optical misalignments, but the process of correcting the pseudo-Planck curve to give the peak sample temperature is model dependent[8]. An alternative method that obviates the need for a spectrometer entirely is multispectral imaging radiometry (MIR[9,10]). In MIR, four near-monochromatic images of the hot sample, each at a different wavelength, are acquired simultaneously on a single CCD camera and then spatially correlated to provide four intensity-wavelength data at each pixel that can be fitted to provide maps of both temperature and emissivity. This method has the advantage over peak-scaling that the temperature of each pixel is determined directly, without recourse to any model dependent parameters. Because each image is focussed independently, chromatic aberration, a potentially important source of uncertainty in temperature measurement is reduced. MIR systems are relatively inexpensive and compact, making them ideal for synchrotron beamlines where space is often at a premium.

MIR has some inherent disadvantages including the challenge of initial optical alignment. The successive halvings of the photon flux due to the sequence of beam splitters also necessitates longer exposure times that can introduce uncertainties due to temporal variations in the temperature field during the acquisition. This ultimately limits the

minimum temperature that can be accurately measured in the original design to ~1700 K[9] (c.f. ~1200 K for spectroradiometry[10]), though a modified MIR system without the ability to independently focus each wavelength has been presented that involves fewer splittings and can achieve accurate temperature measurement down to ~1200 K[11]. MIR also yields larger analytical uncertainties because only four wavelengths are available for fitting (c.f. 1024 for a typical spectroradiometric system[12]). The determination of the system response function is also more challenging, due to the need to aperture the light from the calibration lamp such that the images do not overlap at the CCD. This is especially true when using a source of spectral radiance, where in principle the pinhole would need to be at the surface of the filament itself.

The biggest challenge with the MIR technique however is that of processing the data; the accurate spatial correlation of the four monochromatic images and the need to apply any fitting procedure to ~10k pixels makes this a non-trivial task. Currently, no software specifically designed to perform this processing exists, which could lead researchers to ignore the advantages of MIR over other methods. Consequently we have developed MIRRORS (MultIspectRal imaging RadiOmetRy Software), a new graphical user interface (GUI) for the real-time and post-facto processing of MIR images.

II. DISTRIBUTION

MIRRORS is distributed via an open-source GitHub repository and continues to be developed. The latest release can be downloaded as either a .zip or .tar.gz file from https://github.com/olivertlord/MIRRORS/releases/latest, while bug reports and feature requests can be made at https://github.com/olivertlord/MIRRORS/issues. A listing of previous versions each with a separate citeable DOI and a link to its specific release on GitHub can be found at https://zenodo.org/record/1183326.

A. System requirements

MIRRORS requires MATLAB® and its image, signal and statistics toolboxes to run, and was written and tested on version R2014a running on Microsoft Windows 7 and versions R2015a an R2017a running on Apple OS X 10.13. It will likely work on all versions after R2014a on both Windows and OS X, but has not been explicitly tested. MIRRORS accepts .tiff files of any resolution, aspect ratio and bit depth. Each .tiff file must include four monochromatic images of the hot sample, each centred approximately on the middle pixel of one quadrant of the full image and each at a different, precisely known wavelength. MIRRORS requires a spectral intensity calibration file also in .tiff format produced using a calibrated source placed at the location usually occupied by the sample.

B. Hardware specific code

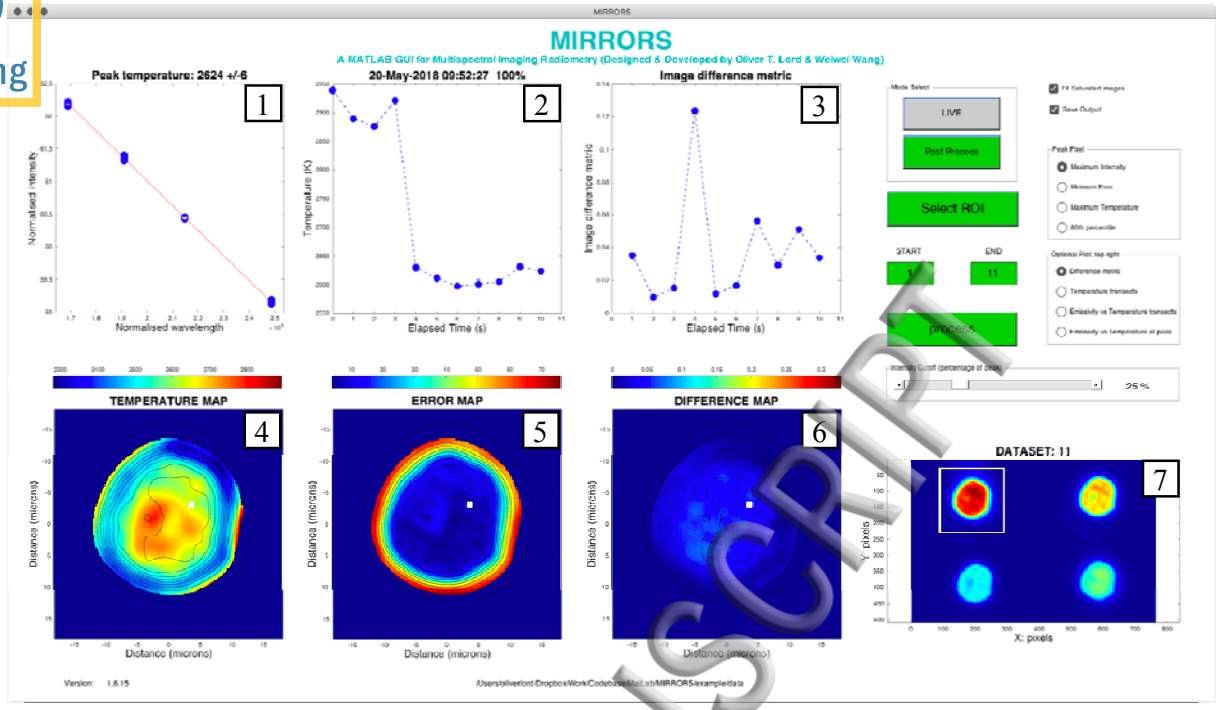

Figure 1: The MIRRORS GUI after data processing has been completed (multimedia view). In this case, the data are from molten Sn surrounded by a KCl pressure medium during laser heating in a DAC at 92 GPa.

While efforts have been made to make MIRRORS universal, some of the code is specific to the MIR system installed at the School of Earth Sciences, University of Bristol which is identical to the system described in Campbell (2008)[9]. Before operation, the wavelengths of the four image quadrants must be changed to the centroids of the bandpass filters employed and the spectral radiance values must be changed to match those of the calibration lamp at those wavelengths. In addition, the magnification and numerical aperture of the optical system and the pixel dimensions of the CCD must be updated. Details of how to make these changes can be found in the README file.

III. WORKFLOW AND METHODOLOGY

The MIRRORS GUI is shown in Fig. 1 and consists of six output plots (labelled 1-6), and a single plot showing the raw input from the CCD (labelled 7) as well as operator controls.

A. Setting up a post-processing task

To run a post-processing task, the user must ensure that the correct spectral intensity calibration file is placed into the /MIRRORS/calibration/ directory with the filename tc.tiff. Clicking the Post Processing button generates a browser window so the user can point MIRRORS to the directory containing the data to be processed. Each file in the folder will be shown in plot 7 sequentially, creating a short movie summary of the experiment. The user can then select an ROI by dragging and then double clicking within the interactive box in the top right quadrant of plot 7, and select the file range to be analysed by entering values into the start and end boxes. Files that contain one or more quadrants with a peak

intensity less than double the intensity of the background are deemed too weak for accurate fitting and are automatically ignored, as are files that contain one or more quadrants with saturated pixels, unless the user ticks the 'Fit Saturated Images' checkbox, in which case MIRRORS will attempt to fit all unsaturated pixels within each image.

A number of additional options are then available to the user. These include a choice between whether the peak temperature reported in plots 1 and 2 is based on the pixel with the maximum intensity (default), minimum error, maximum temperature or the average of all the pixels with intensities above the 80th percentile. The position of this pixel is plotted on the maps as a white square. The user can also choose whether plot 3 shows the image difference metric (default), orthogonal temperature transects centred on the peak pixel, temperature-emissivity transects or the emissivity of the peak pixel as a function of its temperature throughout the experiment. Using the slider control, the user can choose an intensity cutoff below which pixels are not processed, minimising the computational workload and removing areas with erroneous temperatures and emissivities that are the result of fitting pixels where the signal is below the detection limit (usually <10% of the peak intensity). Finally, the user can choose to discard the results of the task by deselecting the 'Save Output' checkbox (the default is to save the data). This option is not available in live mode (i.e. the data are always saved; see below).

To make the interface as user friendly as possible, whenever a required step is complete, the associated button changes colour from grey to green; once all required steps are complete, the 'process' button also turns green. Clicking that button executes the processing routines.

B. Processing Methodology

First MIRRORS divides the calibration image into four equal subframes (Fig. 2a). The same procedure is applied to every unknown image, following a background subtraction step in which the mean of the intensity at the corners of the image is uniformly subtracted from every pixel to remove the contribution of light from the heated sample scattered by the optical system. Extraneous light from outside of the system is effectively eliminated by a light-tight enclosure around the MIR system with a single 10 mm diameter port to allow in the light from the incandescent sample. The CCD software is set to automatically subtract a dark frame from each acquisition to remove the effects of dark current, while readout noise is minimised by setting the thermoelectric cooling on the camera to -20°C.

1. Spatial Correlation

For accurate temperature measurement, it is critical that the subframes of the calibration and unknown images are correlated spatially. Previously, this has been done by manually aligning images such that intensity profiles across a feature recognisable in all subframes were co-incident[9] or by finding the offset between the most intense pixel in each subframe when imaging a backlit ~2-3 μm diameter laser-drilled pinhole[4]. MIRRORS performs spatial correlation automatically on the calibration image and first unknown image of all processing tasks by finding the maximum of the

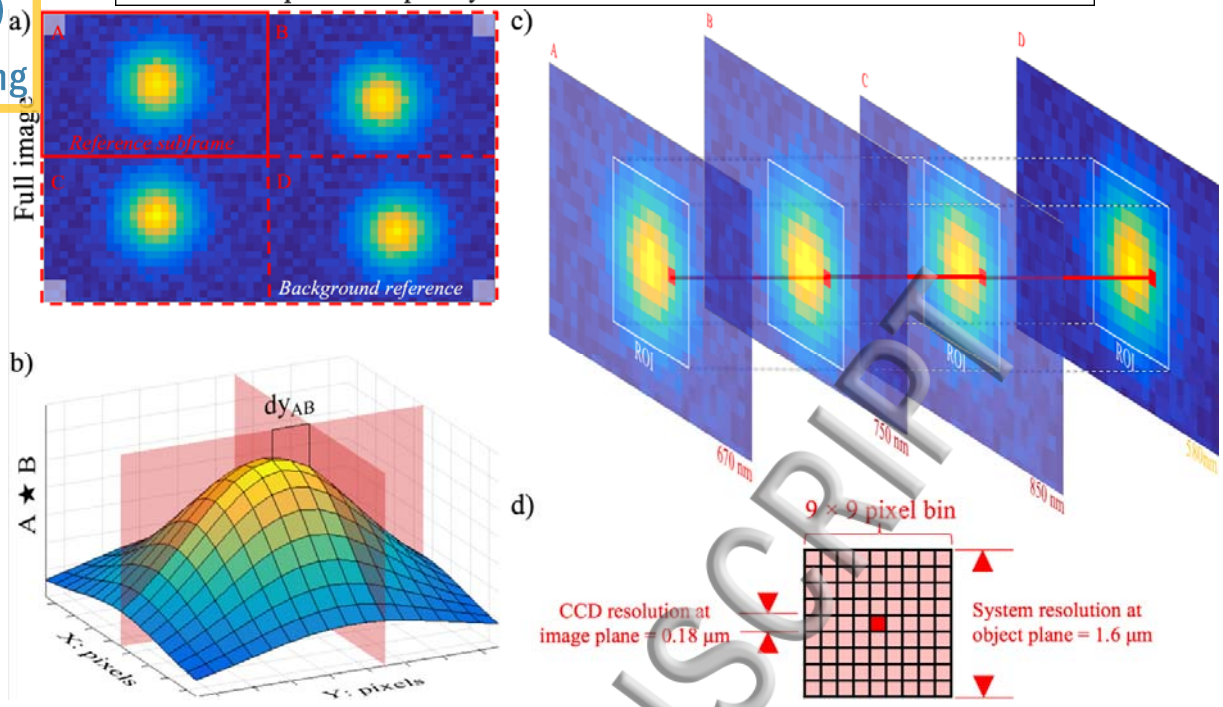

Figure 2: a) Raw CCD image divided into four equal subframes. The white squares represent the locations from which the background is determined. b) The cross-correlation function of reference frame A and frame B. The intersection of the red planes represents the peak in reference frame A; the offset of this point from the peak of the cross-correlation function defines the offset of frame B with respect to A. In this case, $dy_{AB} = 2$ pixels and $dx_{AB} = 0$ pixels. c) Subframes after spatial correlation. The white boxes denote the ROI while the red line connects a single correlated pixel on the sample. d) CCD pixels are binned for temperature fitting with a bin size chosen to approximate the true system resolution.

absolute cross-correlation matrix computed between the reference subframe (the top-left quadrant) and each of the other three subframes using the native MATLAB function xcorr2. This yields three pairs of offset values which are used to shift the subframes relative to the reference subframe in all subsequent unknown images. This procedure is described diagrammatically in Fig. 2a-c.

2. Determination of temperature and emissivity

Each subframe in every unknown image is divided by the equivalent subframe from the spectral intensity calibration image and then multiplied by the spectral radiance of the calibration source at the wavelength of the subframe. This procedure yields subframes corrected for the effects of the optical system on the spectral radiance of the sample. Briefly, the calibration procedure employed at Bristol involves placing an aperture at the object plane of the optical system normally occupied by the sample and focussing a virtual image of the ribbon filament of the NIST calibration source of spectral radiance at the same plane using a pair of plano-convex lenses. The aperture is a rectangle laser cut from 10 µm thick platinum foil with an aspect ratio that matches that of the CCD and dimensions such that the image it produces at the image plane fills each of the quadrants of the CCD completely but without overlap, maximising the useable area of the CCD chip. Temperature, emissivity and their standard error are then determined at each spatially

correlated pixel by fitting the Wien approximation to the Planck function as described in Walter & Koga, 2004[13] to a surrounding bin of pixels from each of the four subframes. This binning is necessary because the CCD resolution at the image plane is likely to be much finer than the true diffraction limited resolution of the system across the fitted spectral range (580 nm - 850 nm) at the object plane (Fig. 2d). MIRRORS determines the required bin size based on the magnification and numerical aperture of the system, the pixel size of the CCD and the Abbé diffraction limit calculated at the midpoint of the fitted spectral range so that the resulting maps are smoothed to match the true system resolution.

3. Image difference metric

MIR affords the opportunity to quantify dynamic changes in the temperature distribution of DAC samples during laser heating often observed subjectively by eye[4]. To do this, MIRRORS computes a difference map by subtracting the current, normalised temperature map from the previous one, and multiplying the result by the normalised intensity map. This multiplier serves to add a greater weight to pixels with higher intensities and lower uncertainties toward the middle of the heated spot where changes, such as melting are expected to occur first. In contrast, contributions from changes in temperature distribution at the edges of the hotspot due to edge effects caused by steep thermal gradients are minimized. This map is then converted into a single non-dimensional metric using equation 1:

$$\delta = \langle |T_{x,y,p} - T_{x,y,c}| \cdot I_{x,y,c} \rangle \quad (1)$$

where the subscripts p and c denote the previous and current maps respectively and $I_{x,y,c}$ is taken from the current intensity map. This procedure was first described in the supplementary information of Briggs et al. (2017)[6] where changes in δ, correlated with sudden drops in peak temperature, were ascribed to percolation of liquid Sn during high pressure melting experiments. A similar feature can be observed in the video associated with Fig. 1.

C. Data output

Once each unknown image has been processed, six output plots are displayed. On the bottom row are maps of temperature (plot 4), its standard error (plot 5) and image difference (plot 6) all overlain with isophotes of normalised light intensity in 10% intervals. On the top left plot is plotted the normalised wavelength-intensity data from the bin surrounding the peak pixel in the current image (denoted by the white square on the maps) and its associated Wien fit (plot 1). On the top middle plot (plot 2) and the top right plot (plot 3) are plotted the peak temperature and image difference metric throughout the experiment both as a function of elapsed time. The radio buttons on the right of the GUI can be used to select alternative outputs for plot 3. The options are orthogonal temperature transects centred on the peak pixel (Fig. 3a) for comparison with traditional spectroradiometric measurements and for easy visualisation of temperature gradients, emissivity-temperature transects (Fig. 3b) and the emissivity of the peak pixel as a function of its temperature throughout the experiment (Fig. 3c). These last two plots can in principal be used to detect phase transitions

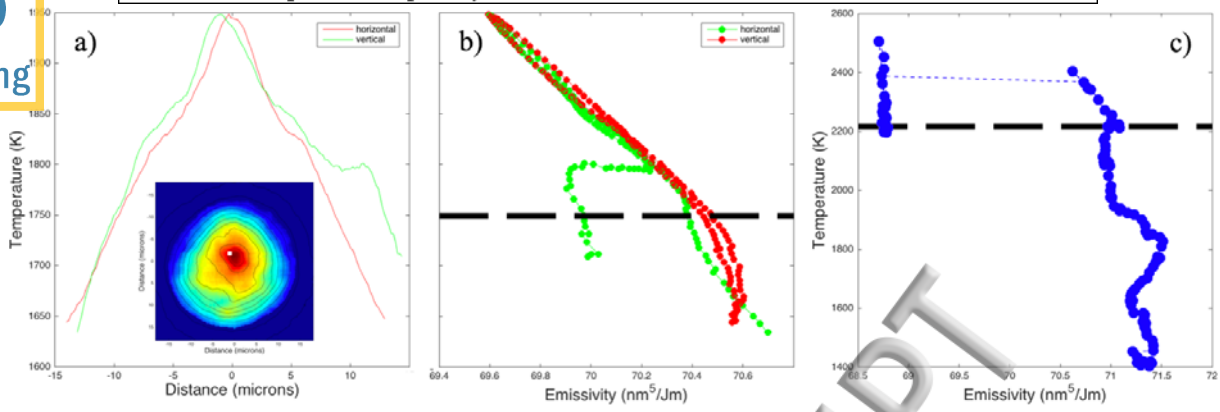

Figure 3: Alternative outputs for plot 3: a) Temperature transects across a steel sample laser heated in air at ambient pressure (see inset for map). Note that the peaks of the transects do not line up because the peak pixel denoted by the white square is set to define the position of the pixel with the greatest intensity and not the highest fitted temperature in this processing. b) Temperature-emissivity transects across the same sample as in a). The dashed line represents the melting point of stainless steel at ambient pressure. c) peak temperature as a function of emissivity during a melting experiment in the LH-DAC on an Fe-S-Si alloy at ~55 GPa. The dashed line represents the solidus from Tateno et al. (2018)[14] at the same pressure.

if the two phases concerned have significantly different emissivity[14]. Fig. 3b shows transects across a stainless steel sample laser heated in air at ambient pressure with a peak temperature of ~1950 K. There is a subtle break in slope at ~1750 K in the vertical transect and one branch of the horizontal transect that matches closely the known 1 atm melting point of stainless steel (the dashed line). Similarly, Fig. 3c shows the emissivity of the peak temperature pixel during a melting experiment on an Fe-S-Si alloy at ~55 GPa. Two distinct trends are seen in the data with a distinct drop in emissivity between the two, as observed at the solidi of pure metals at ambient pressure[15]. The minimum temperature within the low emissivity branch is close to the eutectic melting point of an alloy in the same ternary system recently reported by Tateno et al. 2018[16] on the basis of the appearance of liquid diffuse scattering during *in situ* X-ray diffraction measurements. It should be noted that while these examples show interesting changes in sample emissivity at the known melting point of the material as ascertained from other criteria, emissivity may be a strong function of other attributes and processes, including surface texture, dynamic recrystallisation, liquid convection and chemical reaction between the sample and its surroundings. Consequently, interpreting changes in emissivity as indicative of phase transitions without corroborating evidence is risky[11] and we warn the reader not to take the output of these visualizations at face value but nevertheless include them because of their potential utility in some circumstances.

For each processing task, assuming the 'Save Output' checkbox is ticked, MIRRORS creates a uniquely named folder within the working directory containing a text file for each processed image that lists the temperature, emissivity, their uncertainties and the image difference metric for every pixel position so that all maps can be recreated. At the end of each task, MIRRORS produces a data_SUMMARY.txt file that lists the filenumber, timestamp and elapsed time of each processed image, as well as the temperature and emissivity of the peak pixel, their associated uncertainties and the mean image difference metric. This summary data is also made available to the MATLAB workspace once the task is

complete. Finally, MIRRORS records an animation of the GUI during processing so that the experiment can be replayed without having to reprocess the data.

D. Live Mode

Clicking on the Live Mode button brings up a browser window so the user can point MIRRORS at the folder into which new .tiff files will be saved from the MIR system. As soon as a new file is saved, MIRRORS automatically processes it and outputs the data in exactly the same way as described for post-processing mode, except that the Save Output option is enforced and both the size of the ROI and the value of the intensity cutoff slider control are fixed, to keep computational overheads at a reasonable minimum and thus processing times reasonably short. On a machine with a 3.3 GHz Intel Core i5 processor, MIRRORS will process an image in ~4 seconds. If new .tiff files arrive at a faster rate, MIRRORS will simply catch up by processing the most recent of any batch of new files. Once the experiment is complete, clicking on the Live Mode button a second time executes the same data output procedures that occur at the end of a post-processing job.

IV. BENCHMARKING

To ensure that MIRRORS is working as designed, a set of MIR images and their processed output files are provided as part of the distribution to act as a test of the installation. Details on how to process these images and compare the resulting output against the output provided with the distribution are provided in the README file.

We have extensively benchmarked both MIRRORS and the MIR system at at the School of Earth Sciences,

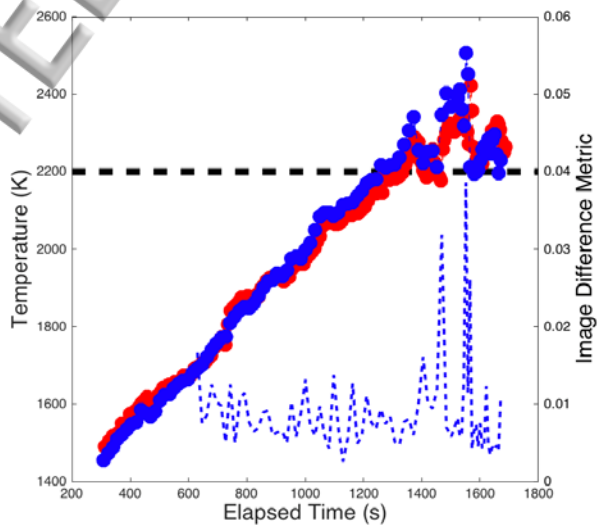

Figure 4: Peak temperature as a function of elapsed time using MIRRORS (blue circles) and spectroradiometry (red circles) during the same melting experiment as described in Fig. 3c. The dashed black line represents the solidus from Tateno et al. (2018)[16] at the same pressure. The dashed blue line is the image difference metric from MIRRORS.

University of Bristol alongside our existing spectroradiometric temperature measurement system. Both systems have similar spectral ranges, share the same optical path up until their branching point and have been calibrated using the same NIST standard of spectral radiance. Files from both systems are timestamped using the same internet based reference clock, and so can be accurately overlain to check for consistency. Critically, the spectroradiometric system has been benchmarked against the known melting points of a range of transition metals in an inert atmosphere at ambient pressure and against high-pressure melting curves of a variety of materials determined using similar systems at different laboratories[17]. It is expected that as long as the entrance slit of the spectroradiometric system is carefully aligned with the hotspot of the sample, the peak temperatures of both systems should be closely co-incident. Fig. 4 is a comparison of the peak temperature of an Fe-S-Si ternary alloy at ~55 GPa in the LH-DAC measured using both spectroradiometry and MIRRORS during a linear ramp of the incident laser power. Below 2200 K, both datasets remain within 40 K of each other due to slight differences in the fitted spectral range and the slight reduction in chromatic aberration afforded by the MIR system. Above 2200 K, the sample is partially molten, as indicated by the plateau in temperature that matches well with the melting curve recently published by Tateno et al. 2018[16] and the two measurements diverge by up 80 K with MIRRORS being the higher of the two. This is due to the fact that the temperature field is undergoing rapid changes in shape such that the hotspot is no longer always aligned with the narrow aperture of the spectroradiometric system, while MIRRORS always captures the peak. A similar comparison can be seen in Lord et al. (2014)[4]. These sudden changes in the shape of the temperature field are clear from the sudden increases in the value of the image difference metric that coincide with sudden drops in peak temperature, as observed for Sn[6].

V. CONCLUSIONS

We have presented MIRRORS, an open source MATLAB GUI designed and developed to process image files generated by a MIR system optimised for temperature measurement in the DAC. MIRRORS can be used in live mode (during an experiment) as well as for post-processing. MIRRORS automates background subtraction, spatial correlation and thermal calibration of subframes within a MIR image and provides the user with maps of temperature, emissivity, their associated uncertainties and an image difference map designed to highlight changes in the shape of the temperature field, as well as a variety of other visualisations derived from them. MIRRORS also produces a video animation of the processing task for later viewing and .txt files containing all of the numerical results so that all of the output plots can be reconstructed in other software. MIRRORS produces nearly identical results to a spectroradiometric temperature measurement system of known accuracy against which it has been benchmarked.

SUPPLEMENTARY MATERIAL

Please see the Supplementary Material for a .zip file containing the code for MIRRORS. A complete distribution of version 1.6.15 of MIRRORS to which this paper relates, including test data and the README file, can be downloaded from https://github.com/olivertlord/MIRRORS/releases/latest.

ACKNOWLEDGMENTS

The authors would like to thank Mike Walter for extensive discussions on all things optical, James Wookey for helpful advice on how to turn ideas into reality in MATLAB and Bob Myhill for discussions on best practice in releasing and documenting scientific software. We would also like to thank the PhD students and post-doctoral researchers in the diamond anvil cell laboratory at the School of Earth Sciences, University of Bristol for detecting bugs and suggesting improvements. We would also like to thank Marissa Wood, who performed one of the experiments reported here. OTL would like to acknowledge support from the Royal Society in the form of a University Research Fellowship (UF150057) and from the Natural Environment Research Council in the form of a post-doctoral research fellowship (NE/J018945/1).

REFERENCES

[1] S. Tateno, K. Hirose, Y. Ohishi, and Y. Tatsumi, Science **330**, 359 (2010).

[2] G. Shen, M.L. Rivers, Y. Wang, and S.R. Sutton, Rev. Sci. Instrum. **72**, 1273 (2001).

[3] O.T. Lord, E.T.H. Wann, S.A. Hunt, A.M. Walker, J. Santangeli, M.J. Walter, D.P. Dobson, I.G. Wood, L. Vočadlo, G. Morard, and M. Mezouar, Physics of the Earth and Planetary Interiors **233**, 13 (2014).

[4] O.T. Lord, I.G. Wood, D.P. Dobson, L. Vočadlo, W. Wang, A.R. Thomson, E.T.H. Wann, G. Morard, M. Mezouar, and M.J. Walter, Earth and Planetary Science Letters **408**, 226 (2014).

[5] A. Kavner and W.R. Panero, Physics of the Earth and Planetary Interiors **143-144**, 527 (2004).

[6] R. Briggs, D. Daisenberger, O.T. Lord, A. Salamat, E. Bailey, M.J. Walter, and P.F. McMillan, Phys. Rev. B **95**, 054102 (2017).

[7] A. Kavner and C. Nugent, Rev. Sci. Instrum. **79**, 024902 (2008).

[8] E.S.G. Rainey and A. Kavner, J. Geophys. Res. Solid Earth **119**, 8154 (2014).

[9] A.J. Campbell, Rev. Sci. Instrum. **79**, 015108 (2008).

[10] M.J. Walter, A.R. Thomson, W. Wang, O.T. Lord, J. Ross, S.C. McMahon, M.A. Baron, E. Melekhova, A.K. Kleppe, and S.C. Kohn, Chemical Geology (2015).

[11] Z. Du, G. Amulele, L. Robin Benedetti, and K.K.M. Lee, Rev. Sci. Instrum. **84**, 075111 (2013).

[12] D. Upadhyay, E.E. Scherer, and K. Mezger, Nature **459**, 1118 (2009).

[13] M.J. Walter and K.T. Koga, Physics of the Earth and Planetary Interiors **143-144**, 541 (2004).

[14] R.A. Fischer and A.J. Campbell, American Mineralogist **95**, 1473 (2010).

[15] C. Cagran and G. Pottlacher, Journal of Non-Crystalline Solids **353**, 3582 (2007).

[16] S. Tateno, K. Hirose, R. Sinmyo, G. Morard, N. Hirao, and Y. Ohishi, American Mineralogist **103**, 742 (2018).

[17] O.T. Lord, M.J. Walter, R. Dasgupta, D. Walker, and S.M. Clark, Earth and Planetary Science Letters **284**, 157 (2009).

MIRRORS

A MATLAB GUI for Multispectral Imaging Radiometry (Designed & Developed by Oliver T. Lord & Weiwei Wang)

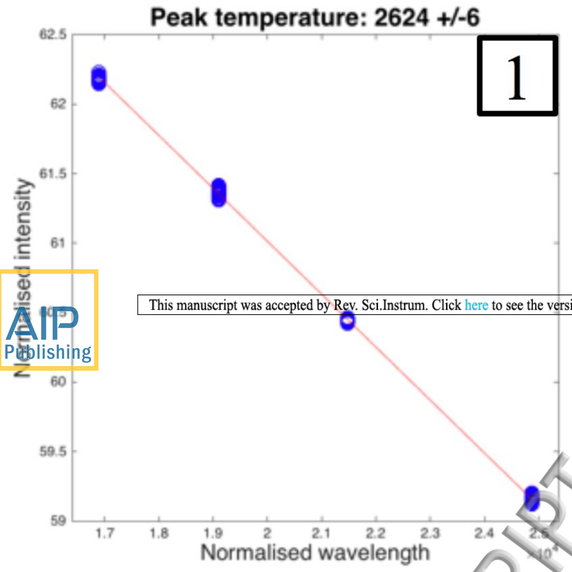

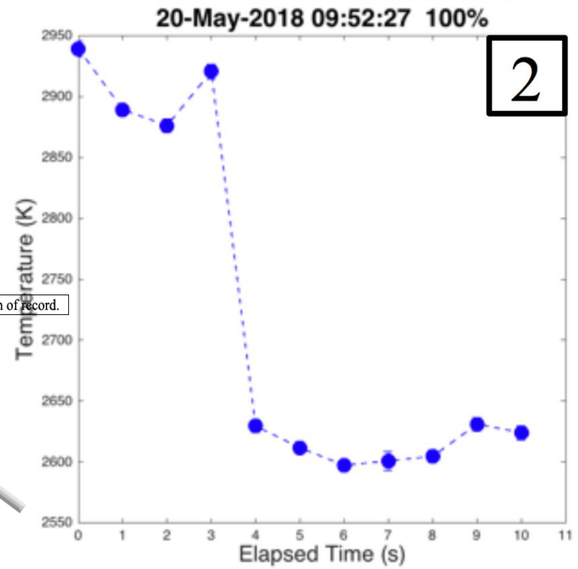

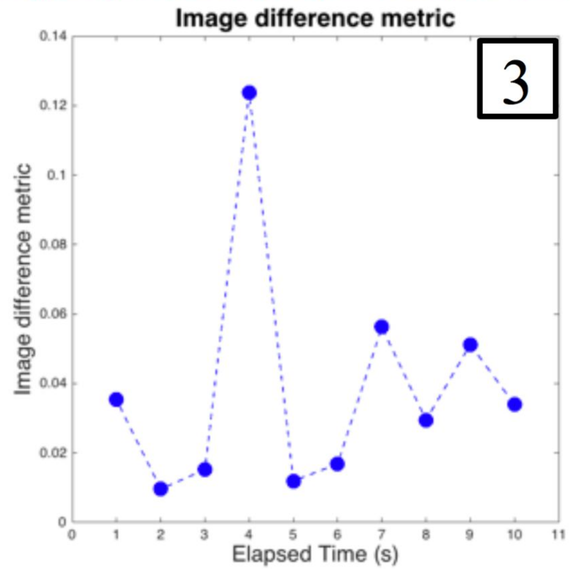

Mode Select

LIVE

Post Process

Select ROI

START 1

END 11

process

Fit Saturated images

Save Output

Peak Pixel

- (•) Maximum Intensity
- ( ) Minimum Error
- ( ) Maximum Temperature
- ( ) 80th percentile

Optional Plot: top right

- (•) Difference metric
- ( ) Temperature transects
- ( ) Emissivity vs Temperature transects
- ( ) Emissivity vs Temperature at peak

Intensity Cutoff (percentage of peak)

25 %

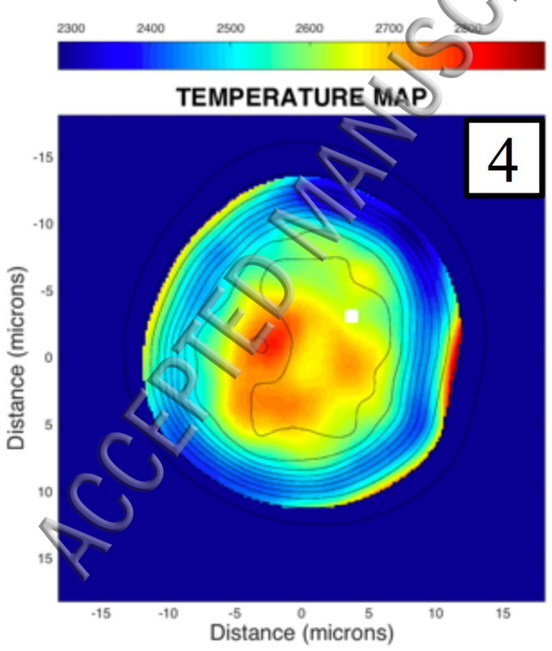

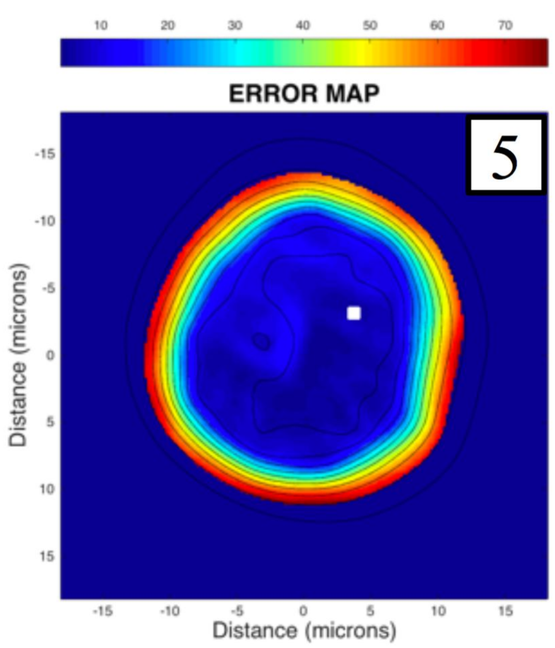

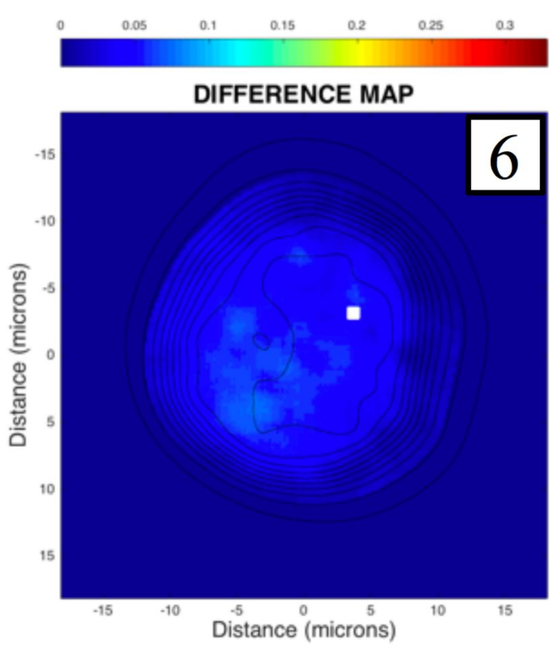

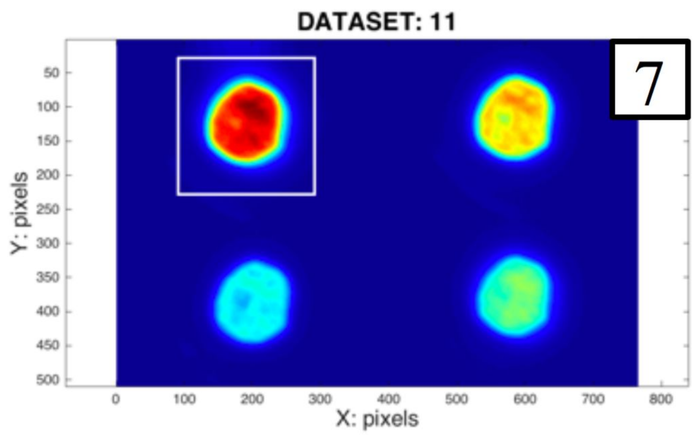

Version: 1.6.15

/Users/oliverlord/Dropbox/Work/Codebase/MatLab/MIRRORS/example/data

a)

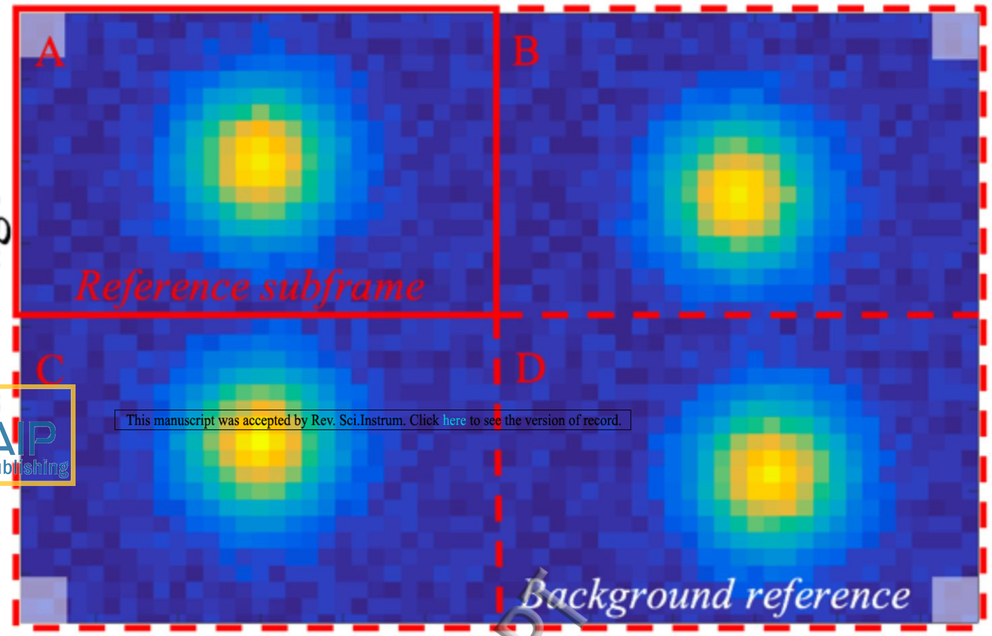

b)

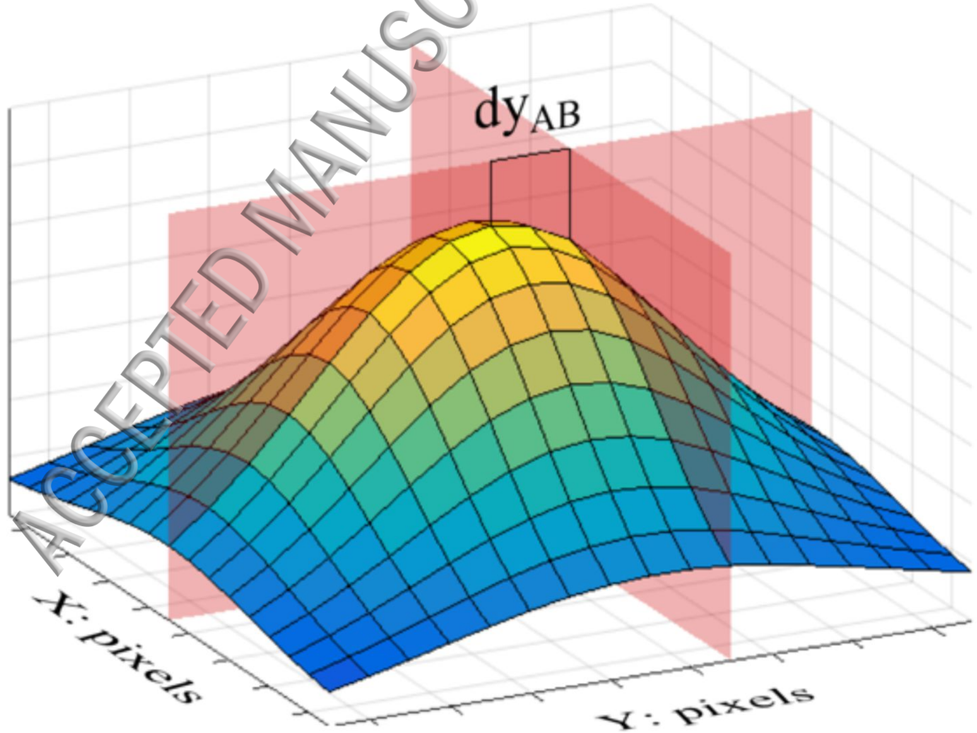

c)

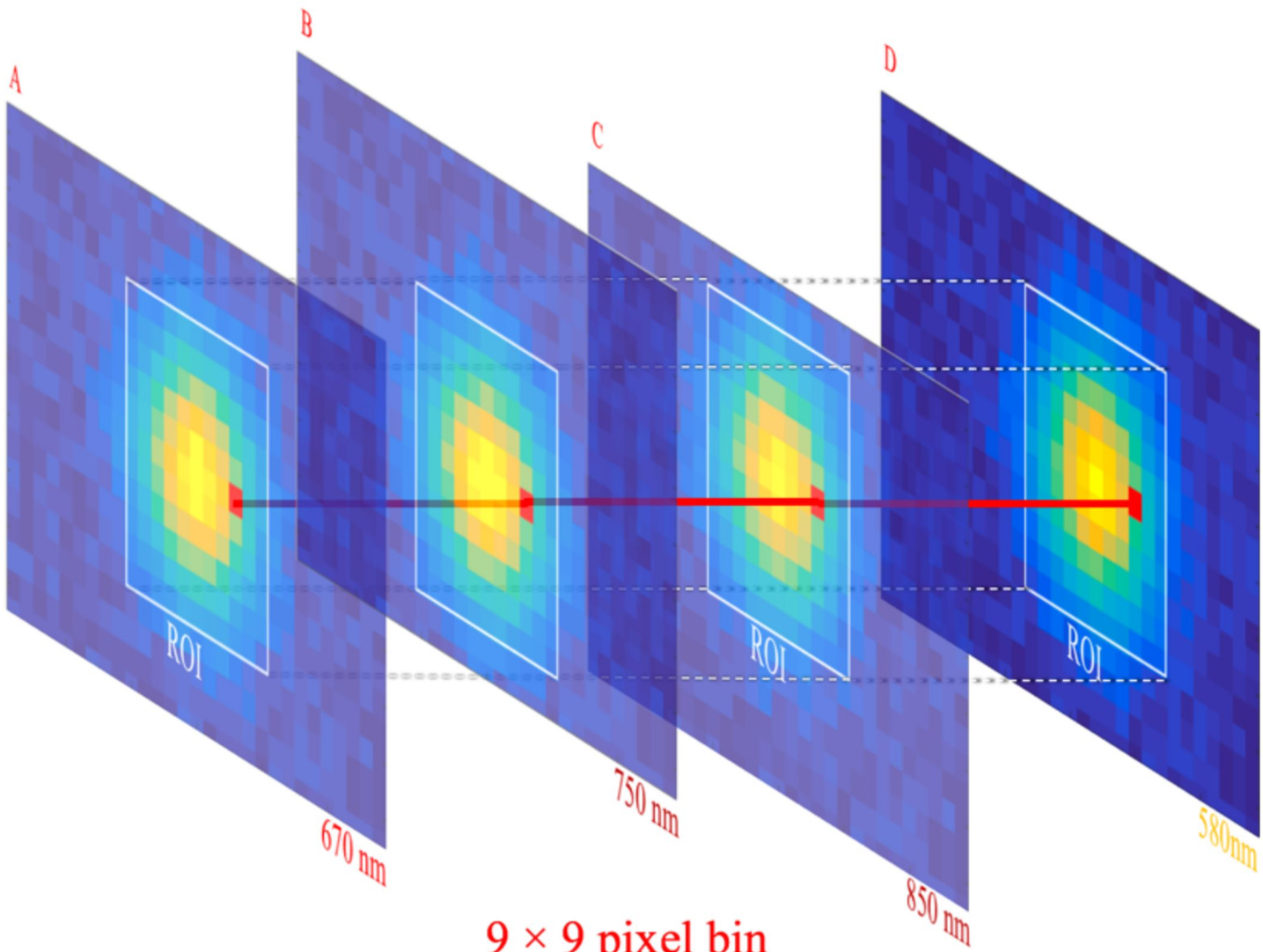

d)